REPORT CTSL– 16

BEAM TRANSFER IN THE CASCADE SYNCHROTRON

ROBERT L. WALKER

JANUARY, 1961

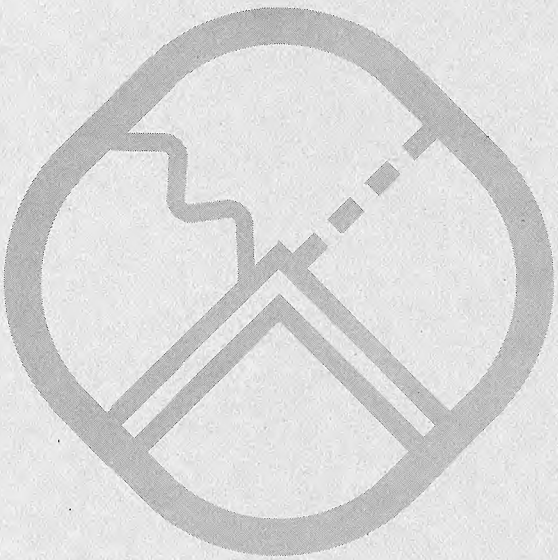

SYNCHROTRON LABORATORY

CALIFORNIA INSTITUTE OF TECHNOLOGY

PASADENA

Report CTSL-16

CALIFORNIA INSTITUTE OF TECHNOLOGY

Synchrotron Laboratory
Pasadena, California

BEAM TRANSFER IN THE CASCADE SYNCHROTRON

Robert L. Walker

January, 1961

Supported in part by the U.S. Atomic Energy Commission
Contract No. AT(11-1)-68

Contents

Acknowledgments

The general ejection scheme described in this report follows closely the corresponding methods proposed by O'Neill for filling storage rings, and by Kuiper and Plass for fast extraction of the beam from the CERN proton synchrotron. Further contributions have been made by E. D. Courant, H. S. Snyder, M. Sands, and A. V. Tollestrup.

BEAM TRANSFER IN THE CASCADE SYNCHROTRON

I Introduction

The problems of beam transfer from the booster to the main ring of the cascade synchrotron[1] may be divided into two classes. The first consists of problems connected with the physical transfer of the beam from the booster ring to the main ring. These problems are: (a) ejection from the booster ring without deterioration of the optical quality of the beam, (b) transport of the beam to the main ring including lenses for matching the region of phase space occupied by the beam to the region appropriate for the main ring, and (c) injection into the main ring.

The second class of problems has to do with the energy matching and R.F. synchronization of the two machines at the time of transfer. These problems will not be discussed in this report.

Of the three problems of physical beam transfer, the ejection from the booster was thought to be the most difficult, and it is the main subject of this report. The general ejection scheme proposed follows the method suggested by O'Neill[2] for transfer of beams from a synchrotron to storage rings. This method has also been proposed for the fast extraction of beams from the CERN and Brookhaven synchrotrons[3].

The general scheme consists of "kicking" the beam through a small angle with a pulsed magnetic field, so that the beam enters a high field "D.C." septum magnet located approximately 1/4 wave length of betatron oscillation later. This high field "bending magnet" then bends the beam away from the booster ring magnets and

---

[1] M. Sands, Synchrotron Laboratory Report No. 10, Calif. Inst. of Tech., September, 1960.

[2] See for example G. K. O'Neill, Report of the International Conference at CERN, 1959, p. 125.

[3] The technical details of the CERN scheme are described in a report CERN 59-30 by B. Kuiper and G. Plass, "On the Fast Extraction of Particles from a 25 Gev Proton Synchrotron".

into the beam transport system. The "kicker" magnet must be pulsed from zero to full field in a time small compared to the circulating period of the particles in the booster ring, and it must be held at nearly constant field for one such period. O'Neill and Korenman[4] have designed delay line magnets for this purpose and both the delay line magnet and other methods are discussed by Kuiper and Plass[3].

The CERN proposal involves physically moving both kicker and bending magnets into place just prior to ejection, in order to reduce the size of the magnets needed and thus the electrical problems of exciting them. We wish to avoid the mechanical problems involved in moving the magnets, especially since a repetition rate of ten per second is envisioned for the booster. This means, of course, larger magnets, but the fact that the energy of the booster is 10 Gev compared to 25 Gev for the CERN machine makes the ejection problem intrinsically less severe. The net result is that the technical problems of exciting the kicker magnets are less severe than those involved in the CERN design for fast beam extraction.

The optical quality of the ejected beam depends on the precision achieved in the magnetic fields of both the kicker and bending magnets, and on the effects of the booster ring fringe fields through which the beam passes. These effects are discussed in Section IV, where it is concluded that extraction may be performed in such a way that very little deterioration of the optical quality of the beam will occur.

The conclusion reached in this report is that it appears quite feasible to extract a beam of good optical quality from a suitably designed alternating gradient synchrotron, so that such a machine can be used as an injector for a higher energy accelerator.

---

[4] O'Neill and Korenman, "The Delay-Line Inflector", Princeton-Pennsylvania Accelerator Project GKO'N 10, VK 3. Dec. 18, 1957. See also References 2 and 3.

II The Booster

The details of the ejection scheme depend on some of the detailed properties of the booster ring such as its lattice structure, wave length, λ, of betatron oscillations, aperture size, and final beam size. Some of these parameters may be chosen in a way to facilitate the beam extraction.

In order to be able to use two or more kicker magnets, it is convenient, although not essential, to have straight sections $1/2\ \lambda$ apart. This result is easily achieved by choosing the number of periods, N, an integral multiple of 2ν, where ν is the number of betatron oscillations per revolution. Further, the kicker and bending magnets should be located $1/4\ \lambda$ apart, or preferably less, so that the above integral multiple should be equal to or greater than 2.

If $\nu = 4.75$, $3(2\nu) = 28.5$ and $4(2\nu) = 38$

The scaling rule $\frac{N}{\nu} = \text{constant}$[1] leads to N = 32.5 and N = 38 for scaling from the Brookhaven and CERN machines, respectively. Thus N = 38 appears to be a reasonable choice. Since perhaps 20 or more straight sections may be desired for R.F. cavities, 3 or 5 for ejection, and several for targets, all 38 straight sections should probably be "long", so that the following simple lattice is reasonable:

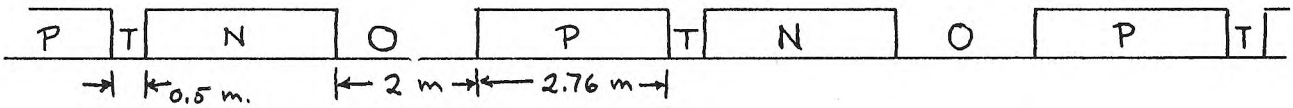

P indicates a section with positive index $n = -\frac{\rho_o}{B_o}\frac{dB}{dr}$.

This produces focussing in the vertical direction and defocussing in the radial one.
N indicates a section with negative n, having the reversed focussing properties.
O indicates a zero field straight section, and T indicates a short zero field transition section.

The above considerations lead to some of the following parameters for the booster. The other parameters are taken from M. Sands: Report SL 10 (ref. 1).

Table I. Booster Parameters

$\nu = 4.75$	
$N = 38$	N = number of periods
$\lvert n \rvert = 103.5$	
$B_{max} = 10$ kg	
$p_{max} = 10$ Gev/c	
$\rho = 33.3$ m.	
$\ell_m = 2.76$ m.	ℓ_m = length per magnet
$C = 305$ m.	C = circumference
$R = 48.5$ m.	
$\lambda = 64.2$ m.	
$\lambda\!\!\!^{-} = 10.2$ m.	
R.F. harmonic, h = 19	

Aperture:

a = 12 cm.	
b = 5 cm.	
$a_{lf} \approx 1.75$ cm.	final beam size*
$b_{lf} \approx 1$ cm.	

The pole contour and the magnetic field shape produced throughout the fringe field region are important for the design of the ejection system. These characteristics are expected to be similar to those of the Brookhaven AGS, although the field gradient resulting from the parameters of Table I is less than that of the Brookhaven machine. The characteristic length, $\ell_o \equiv B_o/\frac{dB}{dr} = \frac{\rho_o}{n}$ is 32 cm for the booster of Table I, compared to 24 cm for the AGS.

The pole contour, the magnetic field B(r) as a function of $r - r_o$, and the field gradient, $G(r) = \frac{dB}{dr}$, as a function of $r - r_o$ are shown for the Brookhaven AGS in Figs. 1 and 2. (The field and gradient are taken from a BNL Memorandum of

---

*The beam size given corresponds to a beam size 3.0 x 1.7 cm in the main ring if the transfer is optically perfect.

January 15, 1959 by J. Palmer and R. Phillips. We are indebted to the BNL group for providing this information.)

III Particle Trajectories During Ejection

In order to reduce the amount of deflection required from the kicker magnets, it is probably useful to displace the equilibrium orbit toward the bending magnet

FIGURE 1.

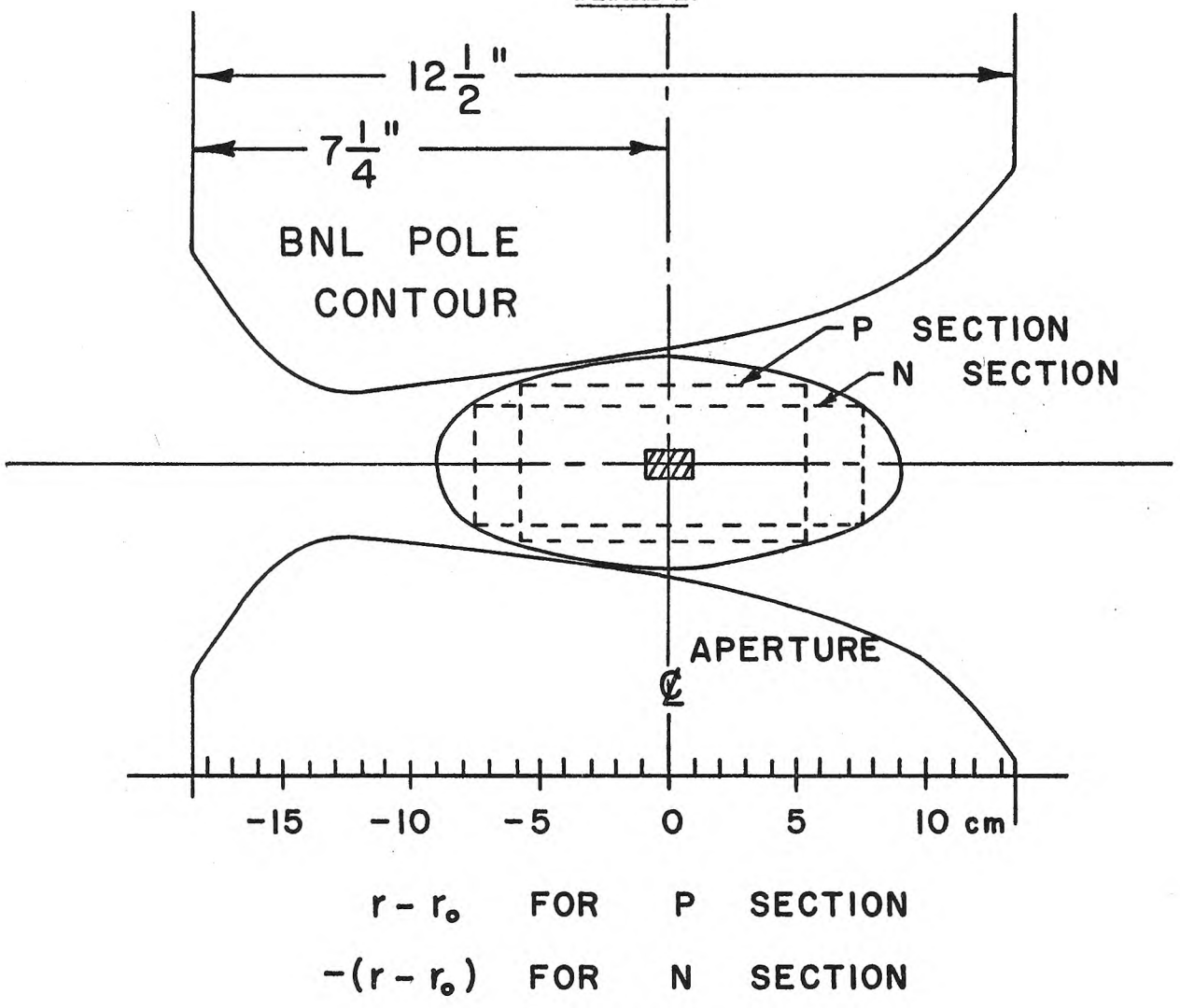

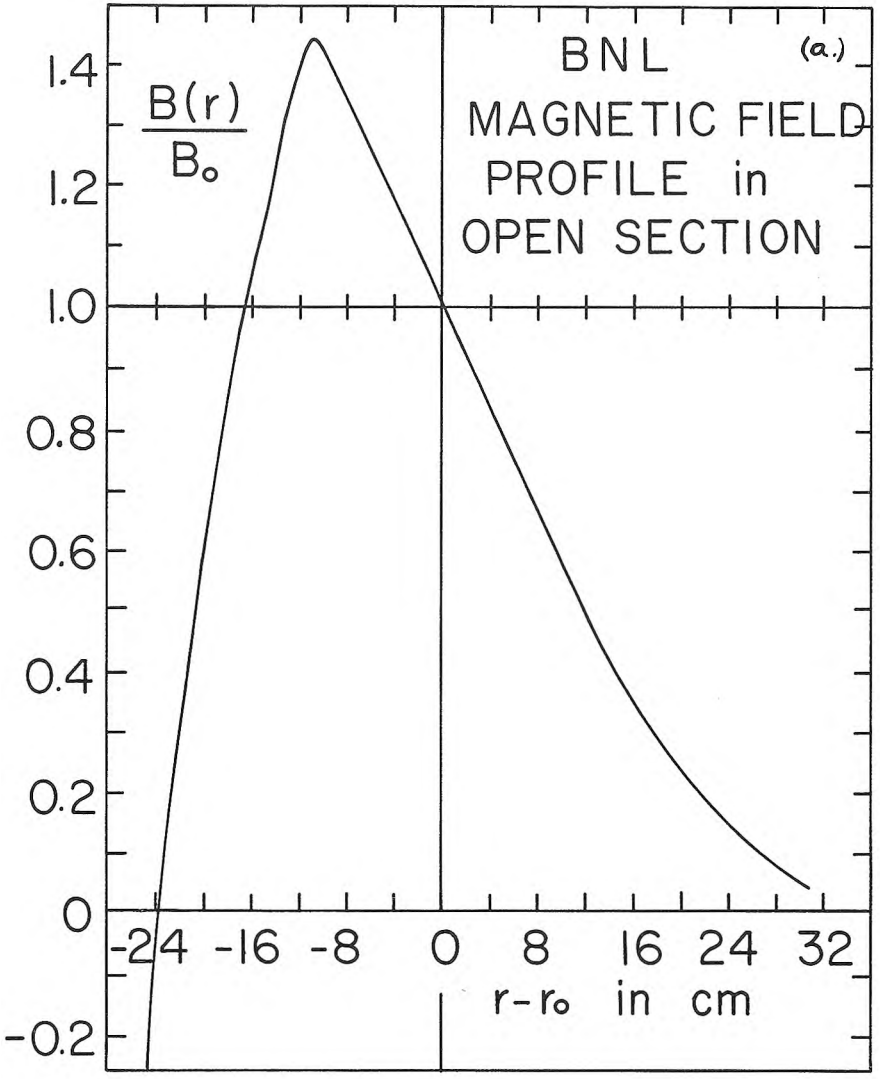
BNL
(a.)
B(r)/B₀
MAGNETIC FIELD
PROFILE in
OPEN SECTION
1.4
1.2
1.0
0.8
0.6
0.4
0.2
0
-0.2
-24 -16 -8 0 8 16 24 32
r-r₀ in cm

FIG. 2

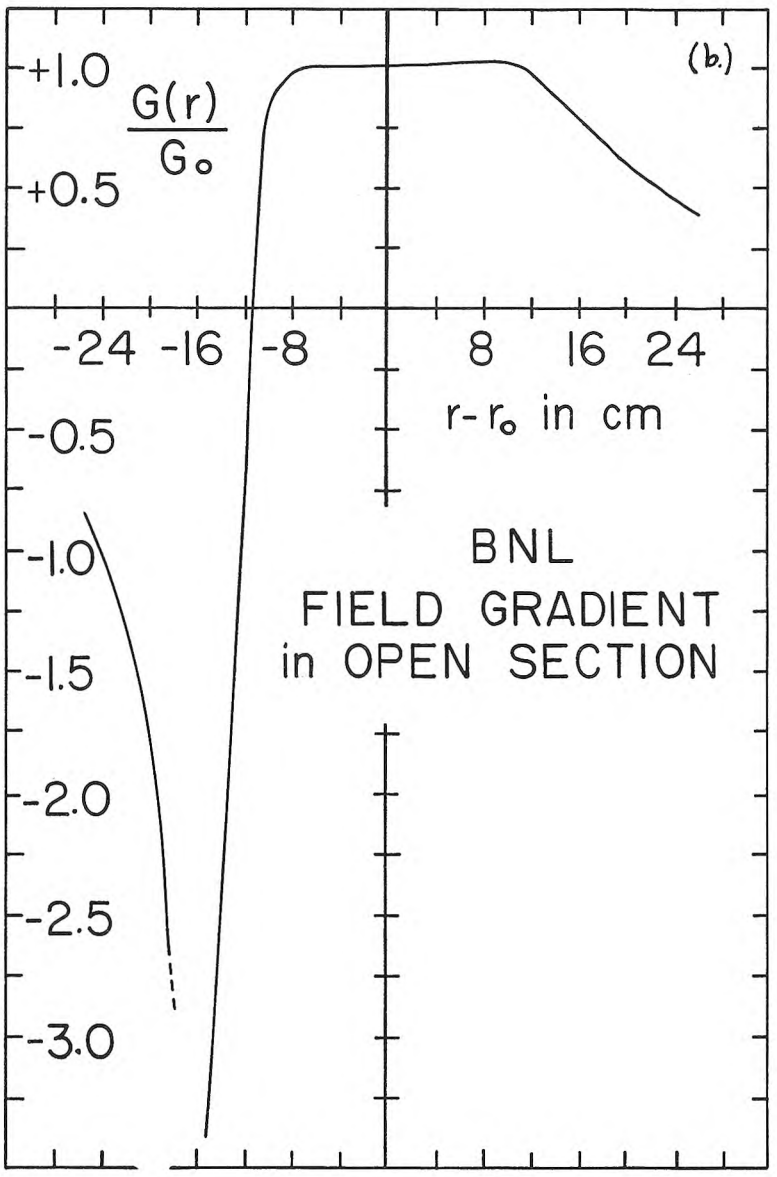
(b.)
G(r)/G₀
+1.0
+0.5
-0.5
-1.0
-1.5
-2.0
-2.5
-3.0
-24 -16 -8 8 16 24
r-r₀ in cm
BNL
FIELD GRADIENT
in OPEN SECTION

shortly before ejection. This might be done by two "orbit deforming" magnets which would be pulsed "slowly" (i.e., with perhaps a 100 μs. period) in such a way as to produce a half-wave-length of betatron oscillation centered at the bending magnet. It might also be done by adjusting the R.F. frequency to move the equilibrium orbit outward throughout the magnet, provided the magnet is made in such a way as to keep the free oscillation frequency independent of radius, so that no resonance is passed in the process. The latter scheme may easily prove to be the most attractive, but in this section, it will be assumed that the first method, using orbit deforming magnets, will be used. For the present purpose, this choice does not make much difference.

The path of the central ray during ejection is shown in Fig. 3, in which the various magnetic field regions are identified by a letter O, P, T, or N indicating the type of field region, and by a number indicating the magnet period. For example, N3 is the negative n section in period no. 3. The orbit deforming magnets, D1 and D2, located in straight sections 04 and 08 produce the deformed path indicated by a dashed curve in Fig. 3a. This is a half period of free oscillation. (A whole period might be used by locating the second magnet, D2, in 012 instead of 08.)

The kicker magnets, K1 and K2, in straight sections 01 and 05 are then pulsed with a pulse rise time of about 0.080 μ sec after which the field should remain constant for 1 μsec, which is the particle circulation period in the booster. (The rise time of 0.080 μsec will sacrifice one beam bunch out of the 19 total.) The kicker magnets will produce the orbit shown by the solid curves in Fig. 3, so that the beam will pass the septum of the bending magnet, B, located in straight section 06. This magnet will then deflect the beam away from the booster magnets and into the beam transport system. (The bending magnet B is pulsed "slowly" with a period of perhaps 100 μs.)

The sum of the angles produced by the two kicker magnets, Ψ, must be 4.0 mrad to produce the path shown in Fig. 3. The angles produced by each of the orbit deforming magnets D1 and D2 must be 4.0 mrad to produce the path shown.

The technical details of the kicker magnets and the bending magnet are discussed in Appendices A and B, respectively. The orbit deforming magnets are trivial and are not discussed.

FIG. 3

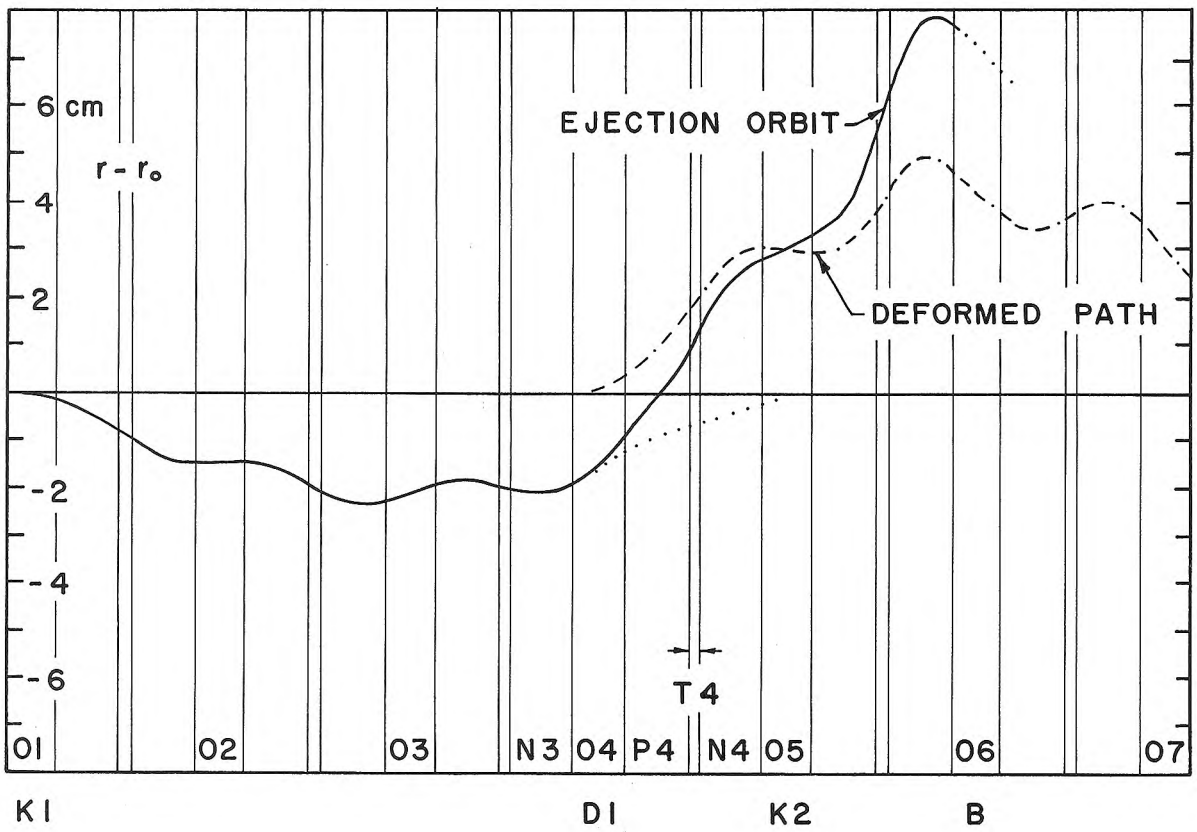
6 cm
4
2
-2
-4
-6
r - r₀
EJECTION ORBIT
DEFORMED PATH
T4
01
02
03
N3
04
P4
N4
05
06
07
K1
D1
K2
B

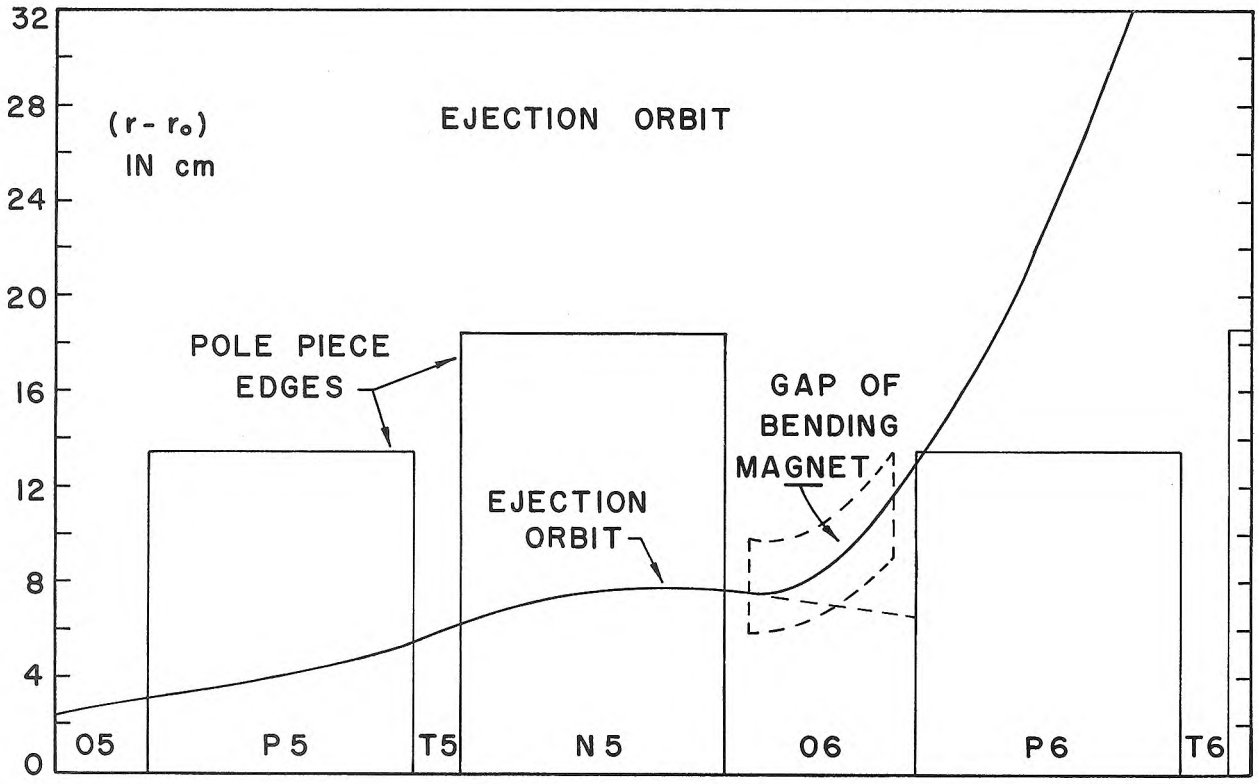
32
28
24
20
16
12
8
4
0
(r - r₀)
IN cm
EJECTION ORBIT
POLE PIECE
EDGES
GAP OF
BENDING
MAGNET
EJECTION
ORBIT
05
P5
T5
N5
06
P6
T6

IV Optical Quality of the Ejected Beam

A very important question concerning the beam transfer system is the extent to which the optical quality of the beam may be spoiled by imperfections in the kicking and b nding magnets, and by effects of the fringing fields through which the beam pass . These questions are most conveniently answered by calculating the region of phase space occupied by the beam at various points along the trajectory. The coordinates of the phase space are x and x', the displacement and angle from the central ray, in either the horizontal plane or the vertical direction. A summary of the focussing properties of various types of magnetic fields and the transformations produced by them in the phase space is given in Appendix C.

(a) Phase Space Regions Occupied by the Beam in the Booster Just Before Ejection.

At any aximuthal position in an alternating gradient synchrotron, the particles of the beam will all lie within some ellipse in the phase space[5]. The shape of the ellipse will vary as the aximuthal parameter, s, varies, but this shape will be periodic with the period L of the magnet structure. This may be stated another way in terms of the transfer matrix, M(s), for one period of the magnet (see Appendix C). If the phase space coordinates, x and $\frac{\rho_o}{\sqrt{|n|}}$ x', form the components of a vector X(s), then one period later, the components will be $X(s + L) = M(s)X(s)$. The periodicity of the limiting ellipse mentioned above is then equivalent to the fact that a point X(s) on this ellipse is transformed by M(s) into another point <u>on the same ellipse</u>. One way of plotting the ellipse is to start with a point X(0) and plot the points $M^n X(0)$ obtained by successive multiplications by M(s). These points all lie on an ellipse which differs from the desired one only by a scale factor. Thus, the proper ellipse at position s is that curve which is transformed into itself by the matrix M(s).

In figure 4 are shown the regions of phase space occupied by the accelerated beam in the booster at the beginning and end of each type of magnet section, for

---

[5] E. D. Courant and H. S. Snyder, "Theory of the Alternating-Gradient Synchrotron". Annals of Physics 3, 1 (1958).

both the radial and vertical oscillations. The ellipses for intermediate points may be found easily from the appropriate transformations given in Appendix C. The ellipse at any azimuth s_2 may be obtained from the one at s_1 by multiplying by the appropriate transfer matrix[5] $M(s_2 \mid s_1)$.

We may now investigate the extent to which the phase space area containing the beam is expanded by imperfections in the kicking and bending magnets and by non-uniform gradients in the fringing field through which the beam passes.

(b) Kicker Magnet Imperfections.

The only appreciable error expected in the kicker magnetic field is a time variation in the field resulting from ripple in the flat top of the pulse. The effects of time variations amounting to $\pm 4\%$ will be calculated here, although it should be possible to achieve greater precision. For example, early tests at Stanford of the delay-line magnets to be used for the Stanford-Pennsylvania electron storage ring experiment[2] indicate that approximately the above precision has already been obtained.

An uncertainty of $\pm 4\%$ in the kicker field will produce an uncertainty of ± 0.16 mrad in the angle produced, or an uncertainty of ± 0.052 cm in the phase space coordinate $\frac{\rho_o}{\sqrt{|n|}} x'$. The effect of including this uncertainty in the phase space region occupied by the beam is shown in Fig. 5. The dashed curve is the normal ellipse for the entrance to section P5 (see Fig. 3) which follows the kicker magnet K2. The solid curve shows the expansion in area required to include the uncertainty in angle. The area is increased perhaps 25%, which, as pointed out above, should be considered an upper limit.

(c) Bending Magnet Imperfections.

Because of the slow pulse, good iron, and ideal geometry of the bending magnet, a high precision should be attainable in the bending magnet field. The precision required in order that the expansion of the phase space area introduced by the bending magnet be the same as that shown in Fig. 5 for the kicker magnets is easily calculated from the fact that the total bending angle is 58 mrad. A variation of ± 0.16 mrad will thus result from field imperfections of magnitude $\frac{\Delta B}{B} = \pm 2.7 \times 10^{-3}$.

FIG. 4 PHASE SPACE OCCUPIED BY THE BEAM IN BOOSTER AT THE END OF ACCELERATION

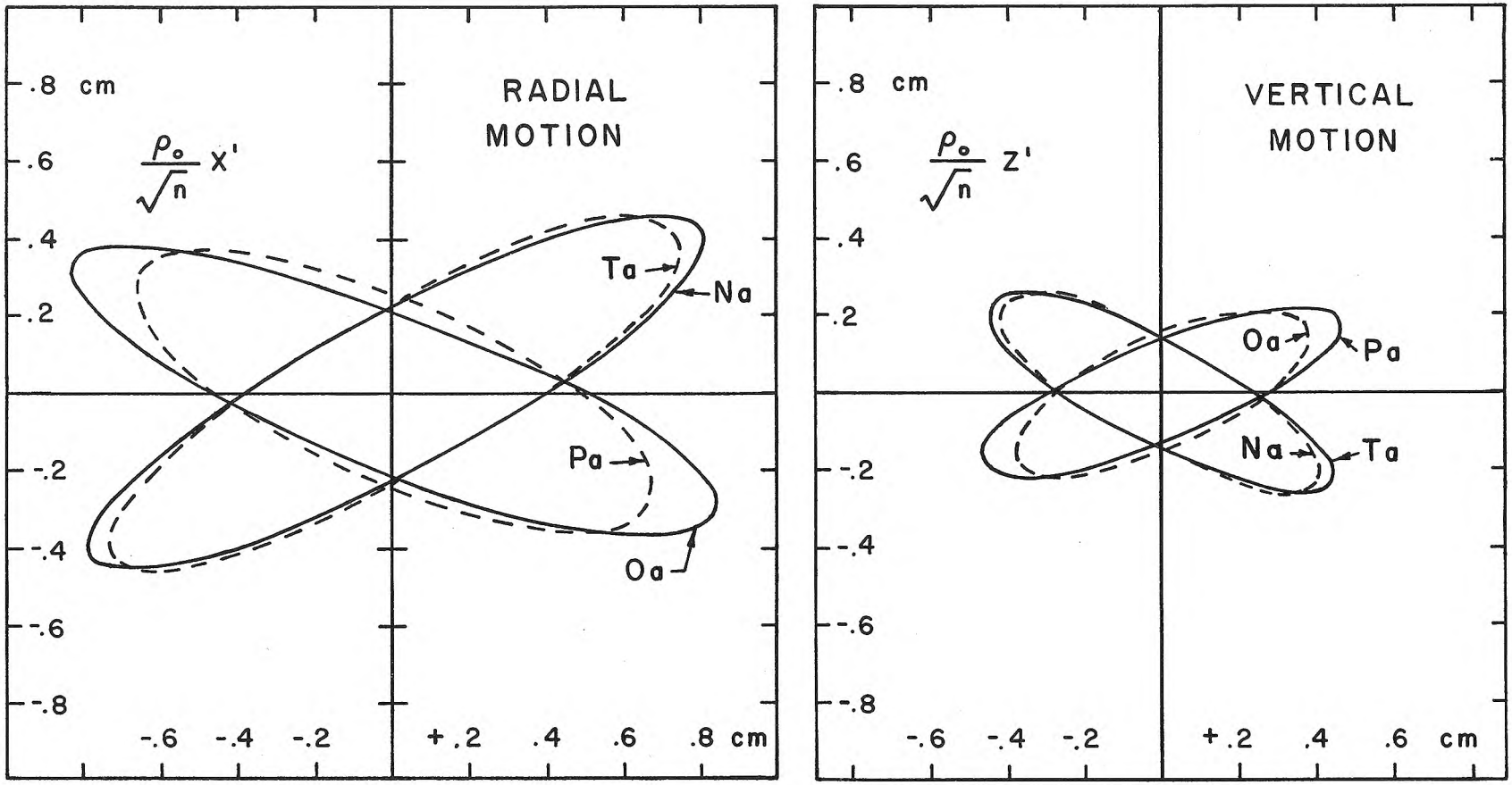

$X = r - r_c$ Z

MAGNET LATTICE IS ···OPTNO··· (Na SHOWS ELLIPSE AT THE ENTRANCE TO AN N SECTION FOR EXAMPLE)

It should be possible to achieve a precision in the field better than the above tolerance, so that no significant deterioration of the optical quality of the beam is expected from the bending magnet. The reproducibility in the field from pulse to pulse can be better than 1 part in 10^3 according to our experience with the pulse transformer injector of the Caltech synchrotron. The field variations over the 1 μs ejection time resulting from the pulse wave form are about 5×10^{-4} as mentioned in Appendix B.

FIGURE 5.

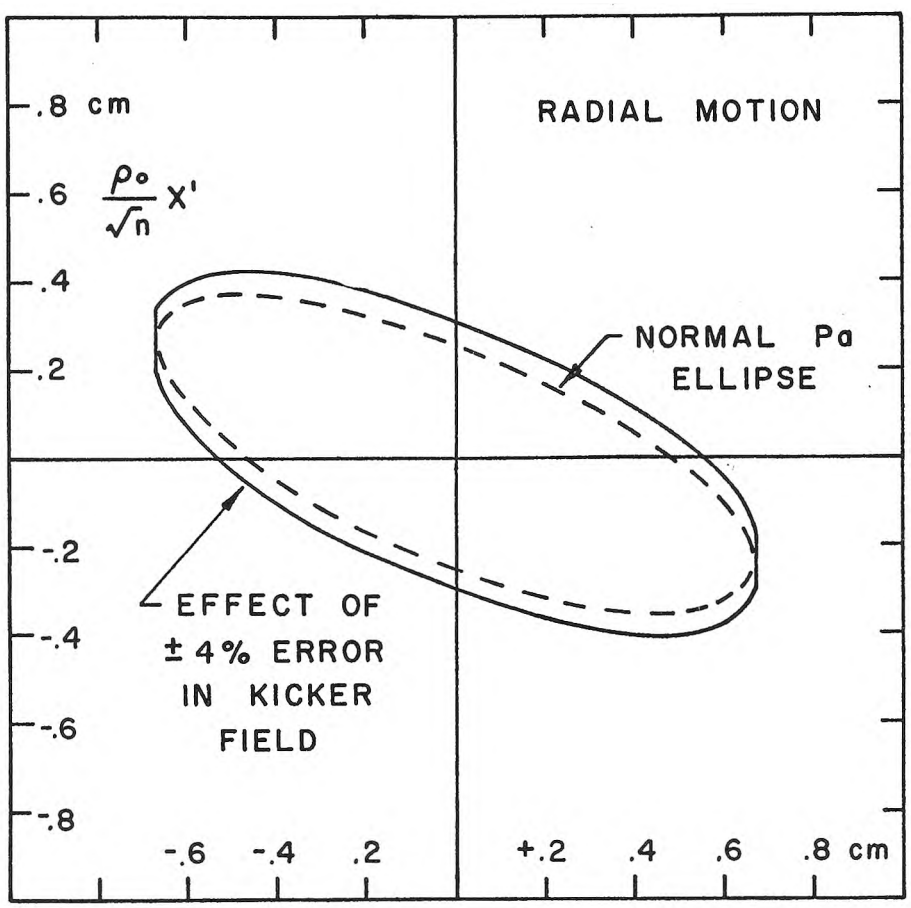

A more difficult thing to estimate is the extent to which the discontinuity in field at the septum winding is not a perfect step from zero field outside to full field inside the septum. An estimate based on the permeability of iron and the geometry of the magnet is that, without taking special precautions, the field just outside the septum would be roughly 3×10^{-3} times the field inside, and variations in the field inside would be somewhat less. By a small current around the entire magnet (i.e., enclosing the return leg) to correct the dipole component of the external field, and possibly by shaping the septum conductor, field errors a few times smaller than the above figure should be possible. Measurements on existing septum magnets would be informative.

The end effects of the magnet are probably important also, and some special shaping of the ends, and possibly the addition "guard" sections might be necessary.

(d) Fringe Field Effects.

The traversal of a region of magnetic field having constant gradient transforms the region of phase space occupied by the beam in the manner described in Appendix C, but does not spoil the optical quality (i.e., an ellipse is transformed into another ellipse). However, if the gradient is not constant over the region occupied by the beam, the phase space area will be bent or twisted into a shape which may be difficult to transform back to an ellipse of the same area. This bent region may be enclosed in an ellipse of larger area for purposes of designing the subsequent optical system. (Actually a "bend" produced at one point on the trajectory could be largely removed at a later point chosen so that the transfer matrix between the two points is ± 1, the unit matrix. However, such a complication in the optical system does not appear to be necessary.)

If the deviation in magnetic field from that corresponding to a constant gradient is δB (see Appendix C, equation 2) we wish to calculate the resulting deviations δx and $\delta x'$ in the phase space coordinates. In first approximation, good if the length of fringe field region is not too long, the error field δB will produce an angular deviation $\delta x'$, without any important change in the position of the trajectory, i.e., δx will be small. In this approximation, the deviation $\delta x'$ may be found very simply by integrating δB along the undistorted trajectory corresponding to uniform gradient.

$$\delta x' = -\frac{e}{pc}\int \delta B\, ds = -\frac{1}{\rho_o}\int \frac{\delta B}{B_o}\, ds$$

If B(x) is expanded in a Taylor series near the central ray, then on the median plane, (z = 0)

$$\delta B = \frac{1}{2} x^2 \frac{dG(x)}{dx}\bigg|_{x=0} + \text{higher order terms.}$$

It is clear that the aberration $\delta x'$ will be proportional to the slope of the field gradient G(x), and this slope is much greater on the "closed" side of the aperture than on the open side, as shown in Fig. 2. The deviation depends also on x^2, i.e., quadratically on the beam size.

According to Fig. 2, the slope of G(x) on the open side of the aperture is: (with lengths in meters)

$$\left|\frac{dG}{dx}\right| \leq 5\, G_o = 5\,\frac{n_o}{\rho_o} B_o$$

then

$$\left|\frac{\delta B}{B_o}\right| \leq 2.5\,\frac{n_o}{\rho_o}\, x^2$$

$$\left|\delta x'\right| \leq 2.5\,\frac{n_o}{\rho_o^2}\, x^2 \ell$$

where ℓ is the length of the path through the fringe field, which from Fig. 3 is approximately 2 meters. If $x_{max} \approx 0.8$ cm as indicated in Fig. 4,

$$\frac{\rho_o}{\sqrt{n}}\left|\delta x'\right| \leq 1.0 \times 10^{-2} \text{ cm.}$$

The distortion in the phase space ellipse of Fig. 4 produced by this small aberration is negligible.

If the beam were to traverse the fringe field for 2 meters in the worst place on the closed side of the aperture, where the slope $\frac{dG}{dx}$ is about 20 times greater, the resulting aberration would be $\frac{\rho_o}{\sqrt{n}}\,\delta x' \approx 0.2$ cm. This would produce an

undesirable distortion of the phase space ellipse, but even in this extreme case, the optical quality would not deteriorate by a really large factor.

The negligible magnitude of the fringe field effect found above makes a more detailed investigation for paths off the median plane unnecessary. It also means that no special effort appears necessary to reduce the slope $\frac{dG(x)}{dx}$ in the region where the beam is brought out. If this were necessary, the field gradient on the open side of the aperture could be maintained approximately constant over a wide region either by the use of a "neutral pole" or an external magnet section producing a negative mirror image field with symmetry plane at $r - r_o = \frac{\rho_o}{n}$, the characteristic length.

In conclusion, it appears that fringe field effects are not serious, and that all effects of the beam extraction system will not result in a deterioration of the optical quality of the beam by more than about 30% in phase space area, corresponding to 10 or 15% increase in the occupied aperture.

V Beam Transport System.

The beam transport system must not only transport the beam from the booster to the main ring, but must also match the phase space occupied by the beam to that appropriate for the main ring.

(a) Phase Space Matching.

The problem of matching the beam to the phase space region appropriate for the main ring is a standard problem which may be solved by various combinations of the four types of magnetic field lenses discussed in Appendix C. Both vertical and horizontal phase spaces must be matched simultaneously. The general problem and a specific solution are described by E. Regenstreif in a CERN report[6], for example. The best method of achieving the match for our specific machine will not be worked out in detail at this time.

---

6) E. Regenstreif, CERN 60-26. July, 1960. "The CERN Proton Synchrotron, 2nd part. Ch. V, Injection".

(b) Beam Transport.

The problems of physical beam transport are not difficult and will also not be worked out in detail. The most economical solution is probably to use a system of thin lenses to solve both the transport and matching problems at the same time. See the CERN report[6] mentioned above, for example.

It might be pointed out that, if desired, the beam may be transported practically any distance in either a curved or straight path by a simple "pipe" which is optically equivalent to the magnet structure of the main ring, i.e., which has the same lattice structure of alternating magnetic gradients. The magnets required for such a pipe would not be expensive, since the aperture required is very small, the field gradients are small, and the fields are constant in time.

(c) Chromatic Aberrations.

The energy spread in the booster beam at ejection time is expected to be so small that chromatic aberrations are unimportant, but it is of interest to estimate their magnitude in order to determine whether the transfer system should be made achromatic.

The energy spread from the linear accelerator for the booster may be decreased to $\Delta T \lesssim \pm 100$ kev by a "debuncher" as described in the CERN report, ref. 6. This gives $\frac{\Delta E}{E} \lesssim \pm 1.0 \times 10^{-4}$ and $\frac{\Delta p}{p} = \frac{1}{\beta^2} \frac{\Delta E}{E} \lesssim 1.0 \times 10^{-3}$. This momentum spread should be damped by a factor of 5 to 10 during acceleration in the booster so that at the time of transfer $\frac{\Delta p}{p} \approx 1$ or 2×10^{-4} from the synchrotron oscillations. The magnetic field in the booster should repeat from pulse to pulse with a precision of better than 3×10^{-4} since the Caltech electron synchrotron magnet repeats with such an accuracy without any unusual precautions. The beam radius at ejection time can probably be controlled to about 0.1 cm, resulting in an uncertainty $\frac{\Delta p}{p} = \frac{1}{\alpha} \frac{\Delta r}{R} = (22.6) \frac{0.1}{5000} \approx 4.5 \times 10^{-4}$. Thus an overall momentum spread $\frac{\Delta p}{p} \approx 5 \times 10^{-4}$ seems reasonable. If, instead of controlling the radius, the final R.F. frequency is fixed, the uncertainty from the radius can be eliminated, and the overall uncertainty will be less.

The dispersion of the bending magnet, which is the main source of chromatic aberration in the ejection system, is

$$\frac{\Delta\theta}{\theta} = \frac{\Delta B}{B} + \frac{\Delta \ell}{\ell} - \frac{\Delta p}{p}$$

where ℓ is the length of path in the magnet. Since $\theta = 0.058$, a spread $\frac{\Delta p}{p} = 5 \times 10^{-4}$ produces an angular spread

$$\Delta\theta \approx \delta x' = 3 \times 10^{-5}$$

or

$$\frac{\rho_o}{\sqrt{n}}\, \delta x' \approx 1 \times 10^{-2} \text{ cm.}$$

This angular spread is negligible on the phase space plot of Fig. 4, so that there seems to be no need to include a chromatic correction in the transfer system, unless it itself involves elements with greater dispersion than the bending magnet.

VI. Injection into the Main Ring

The problem of injection into the main ring is the same as the problem of injecting into any synchrotron and is not specific to the cascade machine. The only difference is the relatively small aperture size of the main ring, which makes the fringe field effects more serious. To find the scaling rule for the aberration $\delta x'$ produced by the fringe field, use the fact that if $\xi = \frac{x}{\ell_o}$ where $\ell_o = \frac{\rho_o}{n}$ is the characteristic length, the relative magnetic field $\frac{1}{B_o} B(\xi)$ is a universal function of ξ. Then

$$\frac{1}{B_o}\frac{dG}{dx} = \frac{1}{B_o}\frac{d^2B}{dx^2} = \frac{1}{\ell_o^2}\frac{1}{B_o}\frac{d^2B}{d\xi^2}$$

and from Section IV d,

$$\delta x' = -\frac{1}{2}\left(\frac{x}{\ell_o}\right)^2 \int \left(\frac{1}{B_o}\frac{d^2B}{d\xi^2}\right)\frac{ds}{\rho_o}$$

The importance of the distortion in the phase space plot such as Fig. 4 may be measured by the dimensionless ratio

$$\frac{1}{x}\frac{\rho_o}{\sqrt{n}}\,\delta x' = -\frac{1}{2}\frac{x}{\ell_o}\int\left(\frac{1}{B_o}\frac{d^2B}{d\xi^2}\right)\frac{\sqrt{n}}{\rho_o}\,ds$$

where the integral now depends only on the fraction of one magnet period integrated over. For example, if the beam passes through the fringe field of one magnet section, the distortion is proportional to $\frac{x}{\ell_o}$. This may be about 4 times larger for the main ring than for the booster, but the resulting distortion is still not serious. However, the increased sensitivity means that the fringe field at the closed side of the aperture must be avoided, and it might be advantageous to extend the region of uniform gradient on the open side by one of the methods referred to at the end of Section IV d.

The large beam size relative to the aperture size means that an injection scheme which is the reverse of the booster ejection scheme is not suitable. A possible injection path is the simple one shown below, where a septum bending magnet in one straight section injects the beam at an angle of about 3 mrad through the fringe field of a P, or positive n, section followed by a long straight section. At the end of the straight section a 1.5 m pulsed kicker magnet supplies a 3 mrad bend to send the beam down the center of the aperture with zero angle. The kicker magnet has a smaller aperture than those in the booster, but needs a slightly larger field, so the electrical excitation problems would not be very different. The precision required of this kicker magnet is slightly higher than that required of those in the booster, but is not unreasonable.

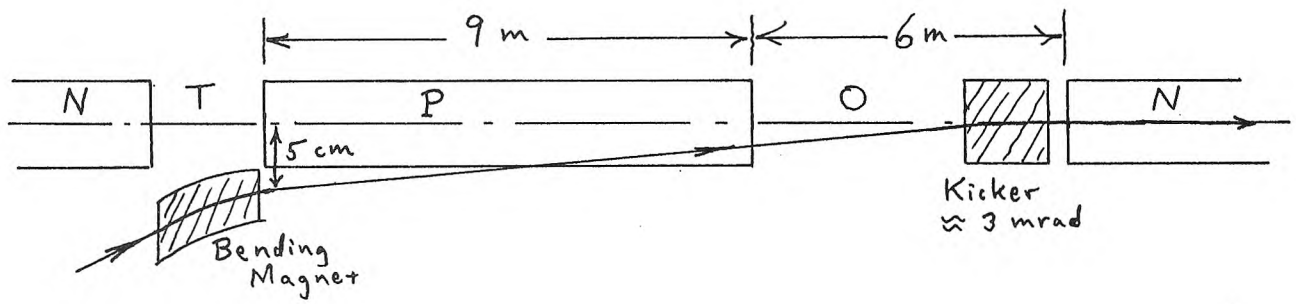

Appendix A. The Kicker Magnets.

The delay line magnet of O'Neill is a one-turn magnet with a ferrite core, having inductance L per unit length and capacitance C per unit length consisting of external capacitors. The magnet is terminated in its characteristic impedance and energized by connecting to a charged line of the same characteristic impedance and a length determined by the length of pulse desired. Then

$$Z_o = (L/C)^{1/2} = \text{characteristic impedance}$$

$$\tau = (LC)^{1/2} = \text{delay per unit length}$$

$$\tau Z_o = L$$

$$V = Z_o I = \frac{LI}{\tau} = \text{voltage required for current I}$$

The two magnet designs below might be considered

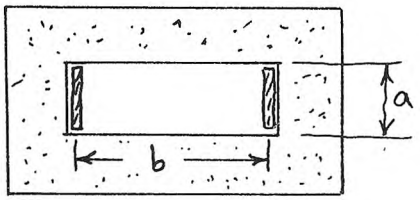

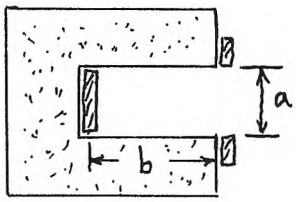

$L = \mu_o \frac{b}{a}$ $\qquad$ $L \approx \mu_o \frac{b + a}{a}$

$\mu_o = 4\pi \times 10^{-7}$ henry/meter = 1.26 μh/m

a = 5 cm	a = 5 cm
b = 15 cm	b = 7 cm for K2
L = 3.8 μh/m	L $\approx$ 3.0 μh/m

The first or closed magnet is probably the one to use since the open magnet is not suitable for K1, and has almost as large an inductance.

A magnet of length ℓ with magnetic field B producing a radius of curvature ρ will give an angle $\psi = \frac{\ell}{\rho}$.

If the particle momentum in Gev/c is

$$p = 0.30\, B\rho \qquad B, \rho \text{ in mks units}$$

then $$B = \frac{p}{0.30} \frac{\Psi}{\ell}$$

$$I \approx \frac{Ba}{\mu_o} (1.15)$$ where the factor 1.15 assumes 15% of the reluctance is in the ferrite.

For $\ell = 3$ m (K1 plus K2), and $\Psi = 4$ mrad.,

$B = 450$ gauss

$I = 2050$ amps

If $V = 50$ kv (which means 100 kv on the line feeding the magnet)

$Z_o \approx 24\,\Omega$

$\tau = 0.16$ μsec/m.

For a rise time of 0.080 μs, the magnet length is

$\ell = 0.50$ meter.

Thus a total of 6 magnet sections must be pulsed simultaneously (3 for each of K1 and K2)

$$C = \frac{\tau^2}{L} = 0.0068 \text{ μf/m.}$$

$P = 103$ MW. = peak power per section

$W \approx 120$ joules = energy per pulse per section

The above parameters might be compared to the CERN proposal for example[3]. One of the CERN designs makes use of a four section kicker with the parameters:

$Z_o = 9.4\,\Omega$

$V = 65$ Kv

$I = 6900$ amps

rise time, 0.05 μs.

Pulse duration, 2.2 μs.

We see that our requirements are significantly less severe. This results mainly from the facts that our energy is smaller by a factor 2.5, our total kicker magnet length is longer by a factor 3, and our rise time is longer by a factor 1.6. On the other hand, our magnet gap is larger by a factor 1.7.

Appendix B. The Bending Magnet.

The bending magnet will be a high field septum magnet constructed of laminated iron and pulsed "slowly" by connecting it to a charged condenser. If the half-period of the pulse is 50 μs, then the field variations during the 1 μs extraction time will be $\frac{\Delta B}{B} \approx \pm 5 \times 10^{-4}$.

The cross section of the magnet is shown below. Parameters of this magnet might be as follows:

a = 2 cm

b = 4 cm

ℓ = 1.5 m = length

B = 13 kg = max. field

ρ = 25.6 m = radius of curvature for a 10 Gev particle.

Ψ = 58.5 mrad = bending angle produced.

I $\gtrsim$ 20,700 amps

L = 3.8 μh = total inductance

W = 815 joules = peak energy in field.

C = 66 μf = capacitance to give 100 μs period.

V $\gtrsim$ 5.0 kv = condenser voltage

F = 1,350 kg/m = force per unit length on the winding.

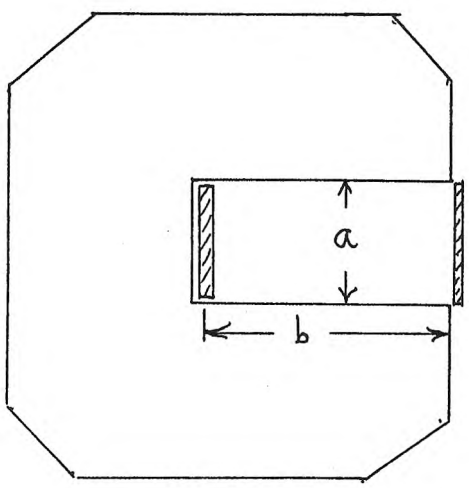

The pressure on the winding producing this force is about 7 atmospheres or 100 pounds/sq.in., which will present some mechanical problems. However, these problems are common to other septum magnet designs, and can presumably be solved. For example, the force on the winding of the proposed CERN magnet[3] would be even greater.

Appendix C. Beam Optics and Phase Space Transformations.

For convenience in discussing the optical quality of the beam in Section IV, a summary is given in this appendix of the focussing properties of various types of magnetic fields and the transformations produced by them in the phase space. (See ref. 5.)

If AB is a particle trajectory, e.g., the central ray, with positions described by the path length s along this trajectory, and $x = x(s)$ is the displacement normal to AB of another particle path in the horizontal plane, then

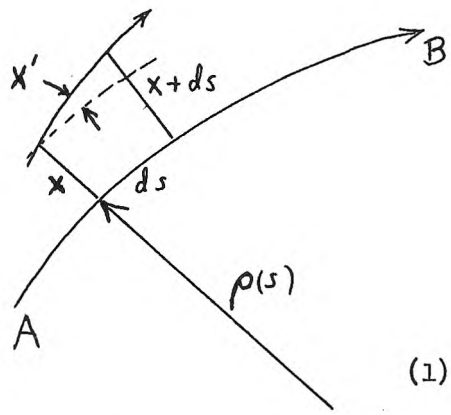

$$\frac{d^2x}{ds^2} = -\frac{e}{pc}\left[B(x) - B(s) + \frac{x}{\rho(s)}B(x)\right] \qquad (1)$$

where $B(s)$ and $B(x)$ are the (vertical) magnetic fields at (s,o) and at (s,x) respectively, and $\rho(s)$ is the radius of curvature of AB at s. Let $B(x) = B(s) + G(s)x + \delta B(x)$ where $G(s)$ is the gradient $\frac{\partial B(x)}{\partial x}$ at $x = 0$ and $\delta B(x)$ is the difference between the actual field and the field corresponding to a constant gradient, $G(s)$, independent of x. Then

$$\frac{d^2x}{ds^2} = -\frac{e}{pc}\left[G(s) + \frac{B(s)}{\rho(s)}\right]x - \frac{e}{pc}\,\delta B(x) \qquad (2)$$

If $G(s) \equiv -n(s)\frac{B_o}{\rho_o}$, $p = p_o = \frac{e}{c}B_o\rho_o$, and $\rho(s) = \rho_o$, then

$$\frac{d^2x}{ds^2} = -\frac{(1 - n(s))}{\rho_o^2}x - \frac{1}{\rho_o}\frac{\delta B(x)}{B_o} \qquad (3)$$

For fields with constant gradient, $n(s) = n$ = constant, $\delta B(x) = 0$, and the solutions of the equation are simple[5].

a) Focussing field: $(1-n) > 0$.

$$x(s) = x(0)\cos\frac{\sqrt{1-n}}{\rho_o}s + x'(0)\frac{\rho_o}{\sqrt{1-n}}\sin\frac{\sqrt{1-n}}{\rho_o}s$$

$$x'(s)\frac{\rho_o}{\sqrt{1-n}} = -x(0)\sin\frac{\sqrt{1-n}}{\rho_o}s + x'(0)\frac{\rho_o}{\sqrt{1-n}}\cos\frac{\sqrt{1-n}}{\rho_o}s \qquad (4)$$

This transformation of $x(0)$, $x'(0)$ into $x(s)$, $x'(s)$ is a clockwise rotation through the angle $\phi = \frac{\sqrt{1-n}}{\rho_o}s$ in the $(x, \frac{\rho_o}{\sqrt{1-n}}x')$ plane. The particles follow circles in this plane, as indicated in the figure. Any area in the phase space occupied by particles will be simply rotated about the origin through the angle ϕ.

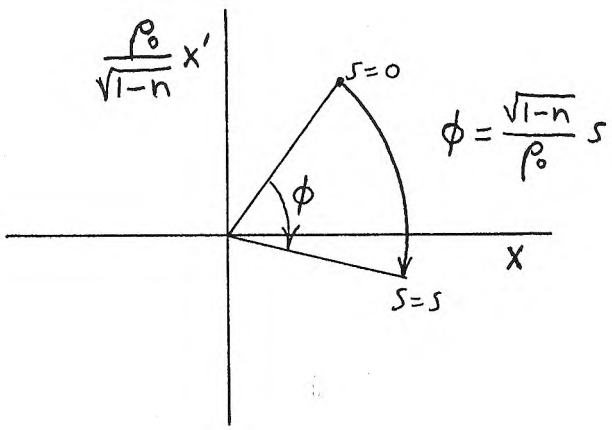

b) Defocussing fields: $(1-n) < 0$

$$x(s) = x(0)\cosh\frac{\sqrt{n-1}}{\rho_o}s + x'(0)\frac{\rho_o}{\sqrt{n-1}}\sinh\frac{\sqrt{n-1}}{\rho_o}s$$

$$x'(s)\frac{\rho_o}{\sqrt{n-1}} = x(0)\sinh\frac{\sqrt{n-1}}{\rho_o}s + x'(0)\frac{\rho_o}{\sqrt{n-1}}\cosh\frac{\sqrt{n-1}}{\rho_o}s \qquad (5)$$

This transformation may also be written:

$$\left[x(s) + \frac{\rho_o}{\sqrt{n-1}}x'(s)\right] = \left[x(0) + \frac{\rho_o}{\sqrt{n-1}}x'(0)\right] e^{\frac{\sqrt{n-1}}{\rho_o}s}$$

$$\left[x(s) - \frac{\rho_o}{\sqrt{n-1}}x'(s)\right] = \left[x(0) - \frac{\rho_o}{\sqrt{n-1}}x'(0)\right] e^{-\frac{\sqrt{n-1}}{\rho_o}s} \qquad (6)$$

In the $(x, \frac{\rho_o}{\sqrt{n-1}}\, x')$ plane this represents an expansion by the factor $e^{\frac{\sqrt{n-1}}{\rho_o} s}$ in the $x + \frac{\rho_o}{\sqrt{n-1}}\, x'$ direction (i.e., along an axis at +45° from the x axis), and a compression by the factor $e^{-\frac{\sqrt{n-1}}{\rho_o} s}$ in the $x - \frac{\rho_o}{\sqrt{n-1}}\, x'$ direction. The particles follow hyperbolic paths in this plane as shown in the figure. The phase space area $\frac{\rho_o}{\sqrt{n-1}}\, x'x$ remains constant.

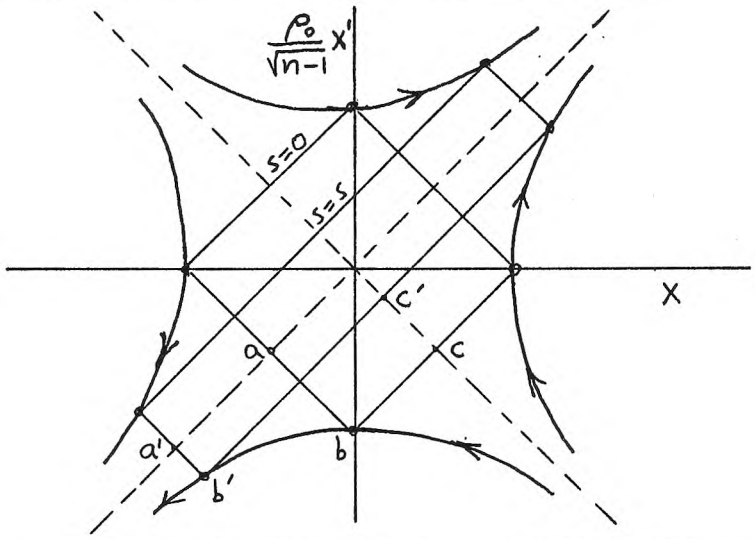

The vertical oscillations are described by solutions of the z equation. These are the same as the x solutions if we replace 1-n by n everywhere. For large $|n| >> 1$, $1-n \approx -n$ and the radial and vertical motions are the same except a radial focussing section is vertically defocussing and vice versa.

c) A region of zero field such as a straight section. B = 0 and

$$\frac{d^2x}{ds^2} = 0 \quad \text{and} \quad \frac{d^2z}{ds^2} = 0 \ .$$

Then

$$x(s) = x(0) + sx'(s)$$
$$x'(s) = x'(0) \qquad (7)$$

This is a horizontal motion in the $\left(x, \frac{\rho_o}{\sqrt{|n|}}\, x'\right)$ plane, through a distance

$$x(s) - x(0) = \frac{\sqrt{|n|}}{\rho_o}\, s \left(\frac{\rho_o}{\sqrt{|n|}}\, x'\right)$$

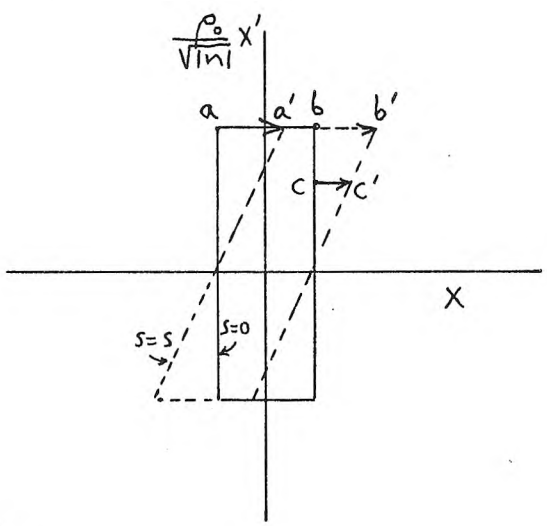

This transformation represents a uniform sheer in the phase space, parallel to the x axis.

d) A thin lens.

A short length of magnetic field will act like a thin lens, i.e., it will produce angle changes without displacement.

$$x(s) = x(0)$$

$$\frac{\rho_o}{\sqrt{|n|}}\, x'(s) = \frac{n}{|n|}\, s\, \frac{\sqrt{|n|}}{\rho_o}\, x(0) + \frac{\rho_o}{\sqrt{|n|}}\, x'(0) \qquad (8)$$

This is a uniform sheer parallel to the x' axis, i.e., a vertical motion through distance $\frac{n}{|n|}\, \frac{\sqrt{|n|}}{\rho_o}\, s$.

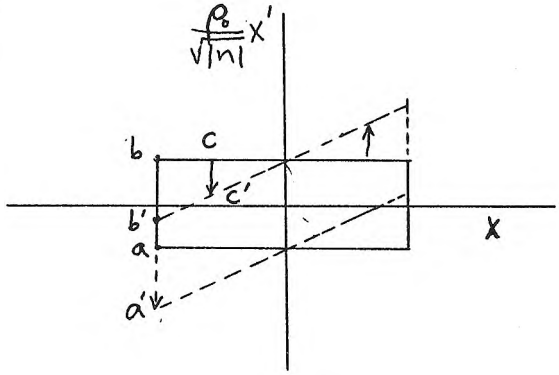

e) Transfer matrices.

The four types of transformations described above may be conveniently represented by matrices which operate on a vector X(0) to give the vector X(s). If the components of X are x and $\frac{\rho_o}{\sqrt{|n|}}\, x'$, the matrices are:

a. $(1-n) > 0$ $\qquad M_a = \begin{pmatrix} \cos\frac{\sqrt{1-n}}{\rho_o}\, s & \frac{\sqrt{|n|}}{\sqrt{1-n}}\, \sin\frac{\sqrt{1-n}}{\rho_o}\, s \\ -\frac{\sqrt{1-n}}{\sqrt{|n|}}\, \sin\frac{\sqrt{1-n}}{\rho_o}\, s & \cos\frac{\sqrt{1-n}}{\rho_o}\, s \end{pmatrix}$

b. $(n-1) > 0$ $\qquad M_b = \begin{pmatrix} \cosh\sqrt{\frac{n-1}{\rho_o}}\, s & \frac{\sqrt{|n|}}{\sqrt{n-1}} \sinh\sqrt{\frac{n-1}{\rho_o}}\, s \\ \frac{\sqrt{n-1}}{\sqrt{|n|}} \sinh\sqrt{\frac{n-1}{\rho_o}}\, s & \cosh\sqrt{\frac{n-1}{\rho_o}}\, s \end{pmatrix}$

c. $B = 0$ $\qquad M_c = \begin{pmatrix} 1 & \frac{\sqrt{|n|}}{\rho_o} s \\ 0 & 1 \end{pmatrix}$

d. Thin lens $\qquad M_d = \begin{pmatrix} 1 & 0 \\ \pm\frac{\sqrt{|n|}}{\rho_o} s & 1 \end{pmatrix}$

The above matrices refer to the "radial" motion. For the "vertical" motion, replace (1-n) by n wherever it appears, and use the opposite sign $\pm$ in M_d.

The matrices are convenient for finding the vector X(s) after a traversal of several successive field regions of different types since the transfer matrix is simply the product of those for the separate regions.